Human Molecular Genetics, 2012, Vol. 21, No. 19 **4286–4300**
doi:10.1093/hmg/dds262
Advance Access published on June 29, 2012

Graded loss of tuberin in an allelic series of brain models of TSC correlates with survival, and biochemical, histological and behavioral features

Elizabeth Yuan[1], Peter T. Tsai[2], Emily Greene-Colozzi[2], Mustafa Sahin[2], David J. Kwiatkowski[1,*] and Izabela A. Malinowska[1]

[1]Department of Medicine, Brigham and Women's Hospital, 1 Blackfan Circle, Room 6-216, Boston, MA 02115, USA and [2]Department of Neurology, The F.M. Kirby Neurobiology Center, Children's Hospital Boston, Boston, MA, USA

Received April 16, 2012; Revised May 21, 2012; Accepted June 25, 2012

Tuberous sclerosis complex (TSC) is a neurodevelopmental disorder with prominent brain manifestations due to mutations in either *TSC1* or *TSC2*. Here, we describe novel mouse brain models of TSC generated using conditional hypomorphic and null alleles of *Tsc2* combined with the neuron-specific synapsin I cre (*SynIcre*) allele. This allelic series of homozygous conditional hypomorphic alleles (*Tsc2*$^{c\text{-}del3/c\text{-}del3}$ SynICre^{+}) and heterozygote null/conditional hypomorphic alleles (*Tsc2*$^{k/c\text{-}del3}$SynICre^{+}) achieves a graded reduction in expression of Tsc2 in neurons *in vivo*. The mice demonstrate a progressive neurologic phenotype including hunchback, hind limb clasp, reduced survival and brain and cortical neuron enlargement that correlates with a graded reduction in expression of Tsc2 in the two sets of mice. Both models also showed behavioral abnormalities in anxiety, social interaction and learning assays, which correlated with Tsc2 protein levels as well. The observations demonstrate that there are graded biochemical, cellular and clinical/behavioral effects that are proportional to the extent of reduction in Tsc2 expression in neurons. Further, they suggest that some patients with milder manifestations of TSC may be due to persistent low-level expression of functional protein from their mutant allele. In addition, they point to the potential clinical benefit of strategies to raise TSC2 protein expression from the wild-type allele by even modest amounts.

INTRODUCTION

Tuberous sclerosis complex (TSC) is an autosomal dominant genetic disease resulting from inactivating mutations in one of two causative genes, *TSC1* and *TSC2* (1). Many clinical manifestations of TSC are due to benign yet often proliferative tumors which develop in multiple organs including the kidneys, lungs, heart and brain. Brain involvement by cortical tubers and other more subtle pathology in TSC is associated with high rates of intellectual disability, learning difficulties, anxiety, attention/hyperactivity disorder and autism spectrum disorders (2–6). The disease has a prevalence of 1 in 6000–10 000 births (7). Less than a third of cases of TSC are of familial inheritance, with the majority of cases resulting from new sporadic mutations. The clinical severity of TSC is highly variable, and the causative mutations that have been identified are equally diverse (8). Most mutations are identified in the *TSC2* gene, and include a variety of missense, in-frame indels, out-of-frame indels, nonsense and splice mutations, as well as large genomic deletions. In addition, there is a small group of missense *TSC2* mutations that are associated with a milder phenotype and have corresponding partial biochemical function (9–13).

The protein products of *TSC1* and *TSC2*, TSC1/hamartin and TSC2/tuberin, respectively, heterodimerize and together regulate cell metabolic activity and cell growth in response to growth factors and changes in nutritional conditions. The TSC protein complex is a key regulator of a conserved serine–threonine kinase, mammalian target of rapamycin (mTOR) (14,15). mTOR occurs in cells in either of two protein complexes, mTORC1 and mTORC2. The kinase activity of mTORC1 is regulated by binding to Rheb-GTP, and mTORC1 phosphorylates multiple substrates, including the S6 kinases (S6K1, S6K2), 4E-BP1 and Grb10 (16,17). Similarly, S6K1 has

*To whom correspondence should be addressed. Tel: +1 6173559005; Fax: +1 6173559016; Email: dk@rics.bwh.harvard.edu

several substrates, including ribosomal protein S6 at sites S235/236 and S240/244, which enhance protein synthesis and cell proliferation. The TSC protein complex plays a critical role in regulating mTORC1 activation by accelerating the hydrolysis of a phosphate group from Rheb-GTP, converting it to Rheb-GDP. Thus, loss of TSC2 causes unregulated, elevated levels of Rheb-GTP and leads to increased mTORC1 activation. The action of mTOR in neurons and particularly in protein translation during synapse formation may affect axon pathfinding and synaptic plasticity (18), contributing to neurodevelopmental abnormalities in TSC patients.

Many previous models of TSC brain disease have been generated in order to evaluate the mechanisms by which TSC loss results in the diverse neuropsychiatric phenotypes noted above. Both *Tsc1*+/− (or k/w) and *Tsc2*+/− mice demonstrate subtle but definite behavioral and electrophysiological abnormalities (19,20). Thus, these observations support the concept that haploinsufficiency of Tsc1 or Tsc2 expression contributes significantly to the brain manifestations of TSC. Using different brain-specific promoters and conditional alleles of *Tsc1* and *Tsc2* (19,21–23), mice in which *Tsc1* or *Tsc2* is lost in neurons or glia have been generated. However, these models display a severe neurologic phenotype including failure to thrive, frequent seizures and early mortality, thereby preventing an evaluation of how brain TSC loss contributes to more complex neuropsychiatric behaviors.

We previously reported the generation of a conditional hypomorphic allele of *Tsc2*, denoted $Tsc2^{c\text{-}del3}$, in which exon 3, which encodes 37 amino acids near the N-terminus of tuberin, is flanked by loxP sites (24). Cre-mediated excision leads to generation of a $Tsc2^{del3}$ allele, which we demonstrated led to the production of a corresponding variant del3-Tsc2 protein at low levels, but of normal function as a Rheb GAP. Several *in vivo* studies demonstrated that the $Tsc2^{del3}$ allele was a hypomorphic allele with some retained function. Homozygous embryos ($Tsc2^{del3/del3}$) survived longer than $Tsc2^{-/-}$ (complete knockout k/k) embryos, but still died by embryonic age 13.5. $Tsc2^{del3/+}$ (d/w) mice developed renal cystadenomas similar to conventional $Tsc2^{+/-}$ (k/w) mice, but at a markedly reduced rate (24).

Here, we report the use of this conditional hypomorphic *Tsc2* allele to develop an allelic series of mice with reduced expression of Tsc2 in neurons to evaluate the correlation between expression levels and phenotype. Remarkably, mice with markedly reduced, but not absent, expression of Tsc2 in neurons had a milder phenotype than mice lacking Tsc1 in neurons, generated with the same Cre transgene. Moreover, with this milder phenotype and improved survival, we were able to examine these mice for behaviors representative of the abnormal clinical TSC phenotype. The severity of these behavioral phenotypes, as well as biochemical and cellular effects, was observed to be proportional to the extent of reduction in Tsc2 expression.

RESULTS

Development of an allelic series of mice with graded reduction of Tsc2 expression in neurons—phenotypic effects

We interbred a conditional hypomorphic allele of *Tsc2* (*c-del3*) and a null allele of *Tsc2* (*k*) with a synapsin I promoter-driven cre recombinase allele (*SynICre*) that has been shown to lead to recombination of loxP sites in neurons beginning at E12.5 (21,25). A mixed colony of these mice was generated from the same founders (Materials and Methods), and mice with two different combinations of alleles were generated: $Tsc2^{c\text{-}del3/c\text{-}del3}$SynICre^{+} and $Tsc2^{k/c\text{-}del3}$SynICre^{+}. Littermate controls were used for all experiments. Hereafter, we denote $Tsc2^{c\text{-}del3/c\text{-}del3}$SynICre^{+} as *Tsc2cc*+, and $Tsc2^{k/c\text{-}del3}$SynICre^{+} as *Tsc2kc*+ for simplicity. Both *Tsc2cc*+ and *Tsc2kc*+ mice were born in Mendelian ratios and were indistinguishable from control littermates until about postnatal day 30 (P30), when failure to gain weight and progressive neurologic phenotypes began to appear. Median survival for *Tsc2kc*+ mice was 89 days, with a maximum survival of 230 days; median survival for *Tsc2cc*+ mice was 137 days, with a maximum survival in excess of 300 days (Fig. 1A). The difference in survival between *Tsc2kc*+ and *Tsc2cc*+ mice was highly significant, $P = 0.0001$, as was the difference in survival between each in comparison with combined littermate controls. Corresponding to their reduced survival, both *Tsc2cc*+ and *Tsc2kc*+ mice demonstrated reduced weight gain in comparison with littermate control mice of the same gender (Fig. 1B). However, *Tsc2kc*+ mice began to show reduced weight gain by 30 days of age (Fig. 1B, bottom), while this difference in weight in comparison with controls took much longer for the *Tsc2cc*+ mice, beginning at age 80 days (Fig. 1B, top). In addition, both sets of mutants had a significant increase in brain weight, in comparison with littermate controls, beginning at age 30 days, with a significant difference between *Tsc2cc*+ and *Tsc2kc*+ mice ($P < 0.05$) seen at age 90 days (Fig. 1C).

We performed formal assessments of neurologic phenotype in these mice beginning at age 30 days. Both *Tsc2cc*+ and *Tsc2kc*+ mice developed abnormal spinal curvature resulting in a hunchback appearance as well as abnormal hind limb posturing when suspended by the tail (Fig. 2A and B). However, both of these clinical features were more severe at all ages in the *Tsc2kc*+ mice in comparison with the *Tsc2cc*+ mice. Neither type of mutant demonstrated Straub tail or tremor at any age, in contrast to our previous experience with the $Tsc1^{cc}$*SynIcre*+ mice, which also had more severe hunchback and hind limb posturing, and a much shorter survival (median 35 days) (21).

On four occasions, the *Tsc2cc*+ and *Tsc2kc*+ mice were observed to have seizures, in the setting of transportation from one portion of the animal facility to another. However, spontaneous seizures were not seen under other circumstances, including in response to noise stimulation and physical manipulation. Mice were often found dead <24 h after being observed to appear normal. No fatal wounds or other major pathology was seen at necropsy to explain sudden death. In addition, use of a lacZ reporter allele demonstrated no recombination outside the brain (heart, lungs, kidneys, liver or other major organs). Since terminal seizure events have been seen in other TSC brain models including $Tsc1^{cc}$*SynIcre*+ mice (21,26), we suspect that terminal seizure events were the main cause of death in these mice.

Neuropathological effects in the *Tsc2kc*+ and *Tsc2cc*+ mice

To understand in greater detail the effects of reduction in Tsc2 expression in these two different mutants, we examined brains

at age 10 days through 90 days (Fig. 3). Progressive neuronal enlargement was seen in both *Tsc2kc+* and *Tsc2cc+* mice. Neuronal enlargement was most obvious in layers IV–V of the cortex probably due to the normally larger size of pyramidal neurons in these layers, but was also seen in all other layers. These enlarged cells were strongly positive by immunostaining with the pS6-S235/236 antibody, consistent with activation of mTORC1 in response to lowered levels of Tsc2. In addition, cells appeared larger and pS6-S235/236 staining was stronger in the *Tsc2kc+* brain sections than in the *Tsc2cc+* brain sections at all ages (Fig. 3). Further, there was a clear progressive increase in the extent of cell enlargement and pS6-S235/236 staining with increasing age, for each of the *Tsc2kc+* and *Tsc2cc+* mice separately (Fig. 3). Reduction in neuronal Tsc2 levels was confirmed by immunostaining in both *Tsc2kc+* and *Tsc2cc+* mice (Supplementary Material, Fig. S1, bottom).

To quantify the neuronal enlargement, we performed blinded measurements of neuronal size in layers IV–V of the motor cortex (M1) on coronal sections (as done previously) (21) (Fig. 4). These data confirmed that pyramidal neurons

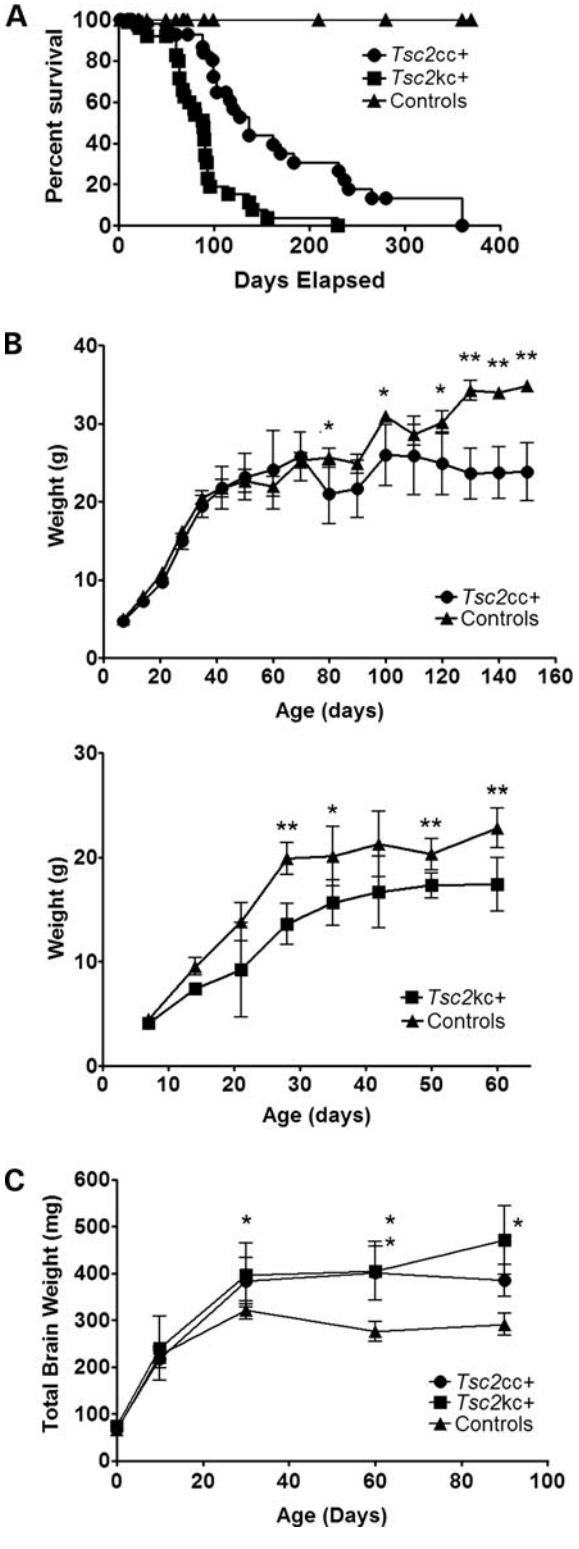

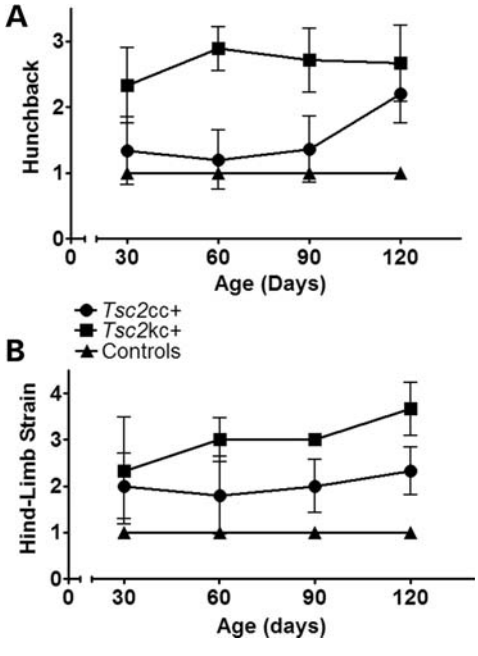

Figure 2. Phenotype scores for *Tsc2kc+* and *Tsc2cc+* mice. Average phenotype severity scores with standard deviations are shown according to age for each type of mutant. $n \geq 3$ for each cohort at each time point, except $n = 2$ for *Tsc2kc+* at age 120 days. (**A**) Severity of Hunchback, scored as: 1, normal; 2, present, mild to moderate; 3, severe. (**B**) Severity of hind limb strain, scored as: 1, normal lateral spread of hind limbs; 2, hind limb shaking and out-of-plane movement; 3, hind limb movement toward midline; 4, clasping of hind limbs.

Figure 1. Survival, weight gain and brain weights of *Tsc2kc+* and *Tsc2cc+* mice. (**A**) The cumulative survival curve of *Tsc2kc+* ($n = 97$), *Tsc2cc+* ($n = 60$) and control ($n = 62$) mice. Median survival of *Tsc2kc+* and *Tsc2cc+* mice is 89 and 137 days, respectively. Pairwise comparison of each survival curve is significantly different ($P < 0.0001$, Mantel–Haenszel test). (**B**) Weight gain in *Tsc2cc+* (top) and *Tsc2kc+* (bottom) mice. Mean and standard deviation are shown. $^{*}P < 0.05$; $^{**}P < 0.001$; by the Mann–Whitney test. $n > 3$ for each cohort at each time point. Equal numbers of male and female mice were used for each genotype. (**C**) Brain weight of *Tsc2kc+* and *Tsc2cc+* mice, and controls. Mean and standard deviation are shown. $^{*}P < 0.05$; $^{**}P < 0.001$; by the Mann–Whitney test in comparison with control mice. $n \geq 3$ for each cohort at each time point, except $n = 2$ for *Tsc2kc+* at 90 days.

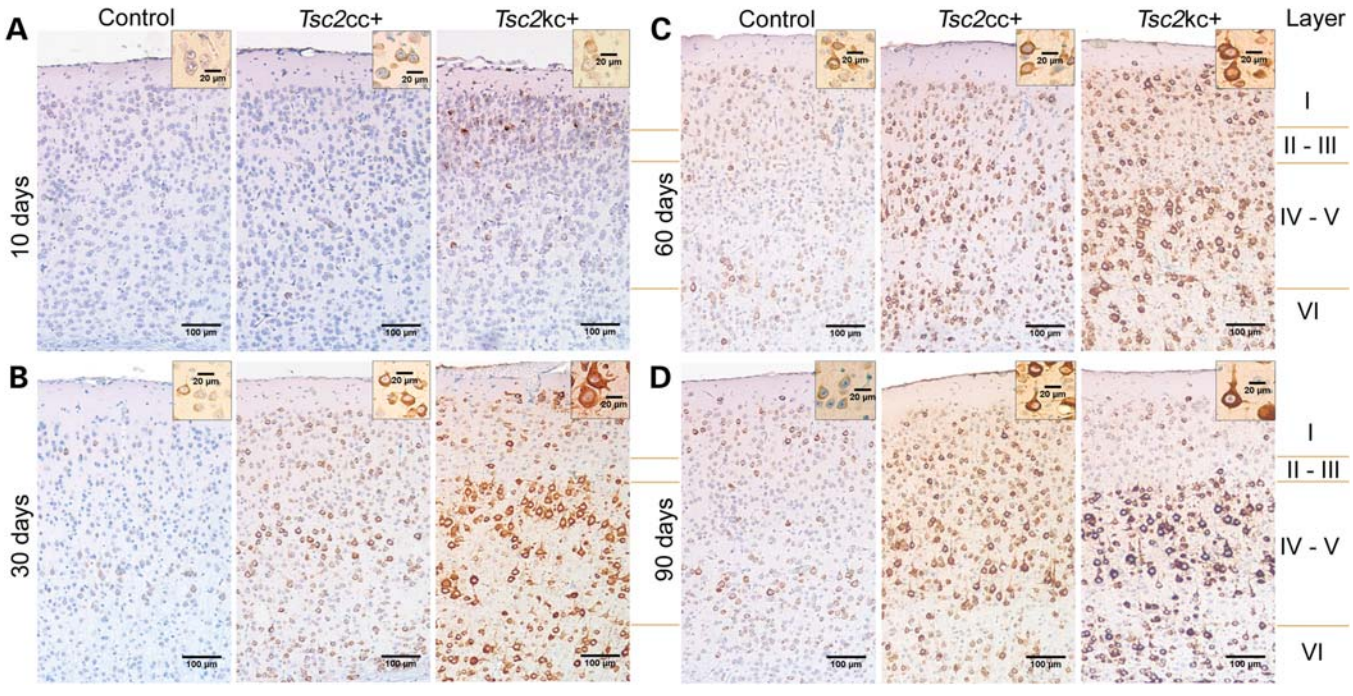

Figure 3. Cortical immunostaining for pS6-S235/236 expression in *Tsc2kc*+ and *Tsc2cc*+ mice. Coronal sections of the M1 region of cerebral cortex are shown for mice of age 10 days (**A**), 30 days (**B**), 60 days (**C**) and 90 days (**D**). Progressively stronger pS6-S235/236 staining is seen predominantly in layers IV and V of both *Tsc2kc*+ and *Tsc2cc*+ mice. At all ages, cell staining and size are greater in *Tsc2kc*+ than in *Tsc2cc*+. Insets show the largest cells seen in these fields at higher magnification. Scale bars in large images are all 100 μm; in small insets are 20 μm.

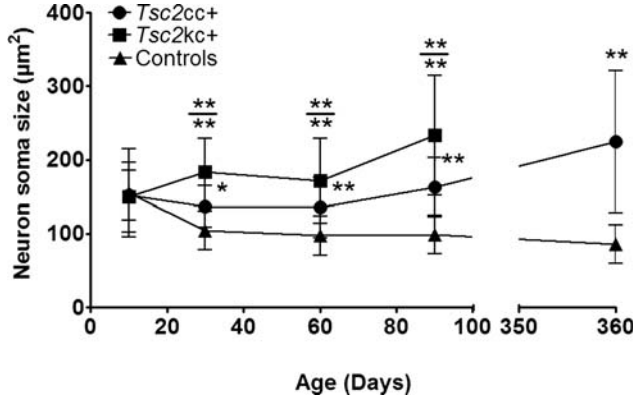

Figure 4. Neuron soma size in *Tsc2kc*+ and *Tsc2cc*+ mice. Average neuron soma size with standard deviations are shown according to age for each type of mutant. Neurons were measured in layers IV–V of the M1 region of cerebral cortex. $^{*}P < 0.05$; $^{**}P < 0.001$; by the Mann–Whitney test. Asterisks above a data set indicate comparison with control mice; asterisks above the bar (at top) indicate comparison between *Tsc2kc*+ and *Tsc2cc*+. $n \geq 2$ mice for each cohort at each time point.

from these layers were significantly larger in *Tsc2kc*+ mice than in those from *Tsc2cc*+ mice, which were correspondingly significantly larger than those in controls ($P < 0.001$ for each comparison at ages 60 and 90 days). In addition, there was progressive enlargement of neurons in both mutants through age 90 days, which continued up to age 360 days for the *Tsc2cc*+ mice.

We also examined the hippocampus in *Tsc2kc*+ and *Tsc2cc*+ brains at 60 days of age. In all hippocampal regions, CA1, CA3 and dentate gyrus, we found neurons that were strongly positive for pS6-S235/236 expression by immunohistochemistry (Fig. 5). In addition, increased numbers of pS6-S235/236+ ectopic neurons were seen in the stratum oriens (above CA1) in both *Tsc2kc*+ and *Tsc2cc*+ mice (1.93 ± 0.08, 1.44 ± 0.21, 0.45 ± 0.25 pS6+ cells per 0.01 mm^2, respectively, for *Tsc2kc*+, *Tsc2cc*+ and littermate controls; $P < 0.003$ for each comparison), similar to previous observations in *Tsc1*^{cc}*SynICre*+ mice (21). Marker allele studies, using a lacZ reporter allele, indicated that recombination had occurred exclusively in neurons in these same regions (Supplementary Material, Fig. S2).

Other regions of the brain, including the thalamus and hypothalamus, also showed a qualitative increase in neuronal cell size in the mutants. We also examined spinal cord anterior horn motor neurons in the mutants, and found that they also showed an increase in cell size and a corresponding decrease in Tsc2 protein expression (Supplementary Material, Fig. S3). Quantitative analysis showed that these differences were highly significant, $P < 0.001$ (Supplementary Material, Fig. S4).

Assessment of Tsc2 loss and mTORC1 activation in brain lysates and quantification of recombination

Immunoblotting was performed to assess semi-quantitatively the reduction in Tsc2 levels and mTORC1 activation in the brains of these mutant mice (Fig. 6). The expected decreases in Tsc2 levels, and increases in mTORC1 signaling were observed, which appeared qualitatively to become worse

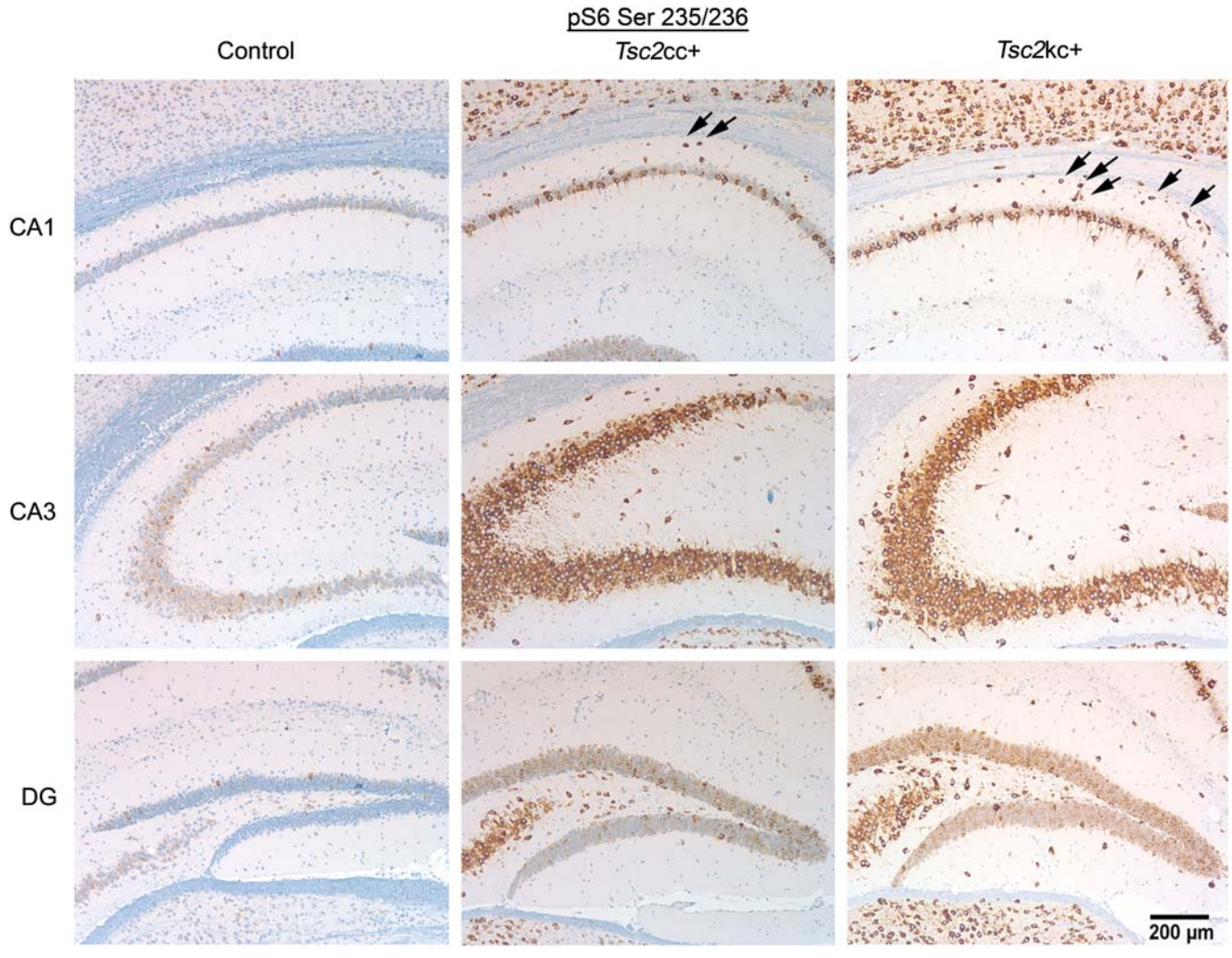

Figure 5. Expression of pS6-S235/236 in the hippocampus of *Tsc2cc+* and *Tsc2kc+* mice. Immunohistochemistry images are shown for control, *Tsc2cc+* and *Tsc2kc+* mice at 60 days of age. pS6-S235/236 strongly positive neurons are seen in both *Tsc2cc+* and *Tsc2kc+* sections. Note the presence of ectopic pS6-S235/236+ cells in the stratum oriens (arrows between cortex and CA1) of both mutants. The scale bar is 200 μm for all images. Hippocampus regions: cornu ammonis 1 (CA1), CA3, dentate gyrus (DG).

with age, in comparing mice of ages 30 and 90 days (Fig. 6A). To provide more quantitative information, we compared the ratios of expression of several proteins of interest in mouse brain lysates at age 90 days (Fig. 6B). Tsc2:GAPDH levels were reduced to 20 and 35% of normal in *Tsc2kc+* and *Tsc2cc+* mice, respectively, with each comparison with controls significant at $P < 0.02$. Consistent with this reduction and observations in Figure 3, levels of pS6-S235/236:S6 and pS6-S240/244:S6 were both significantly increased in both *Tsc2kc+* and *Tsc2cc+* mice, in comparison with controls. In addition, pAkt-S473:Akt levels were significantly reduced in both genotypes. Note that all of these values were more distorted in *Tsc2kc+* than in *Tsc2cc+* mice, but were not significantly different comparing those two groups for any of them individually. However, the trend was uniform, and for the comparison between Tsc2:GAPDH levels in the two mutants, the difference was nearly significant, with $P = 0.063$.

To extend these findings, we performed two additional studies. First, we developed a quantitative multiplex ligation probe-dependent amplification (MLPA) assay to determine the relative levels of *Tsc2 c-del3*, *del3*, *w* and *k* alleles in a DNA sample (see Materials and Methods and Supplementary Material, Fig. S5 for details). This assay permitted quantification of the relative amount of conversion of the *c-del3* to the *del3* allele in cortical samples from the *Tsc2kc+* and *Tsc2cc+* mice (Supplementary Material, Fig. S6). Analysis of cortical samples at a range of ages from 0 to 90 days indicated that recombination was seen in about 10% of *c-del3* alleles at age 0, increased to about 20% at age 10 days and reached 35% recombination at age 30 days, and remained stable thereafter. These observations are in accord with expectations, given that although recombination is occurring in the majority of neurons due to activity of the synapsin I promoter, there are multiple other cell types in the brain. These observations suggest that recombination of the *Tsc2 c-del3* allele to the *Tsc2 del3* allele was complete by age 30 days, and that delayed recombination did not account for the progressive decline in the proportion of Tsc2 protein in brain lysates

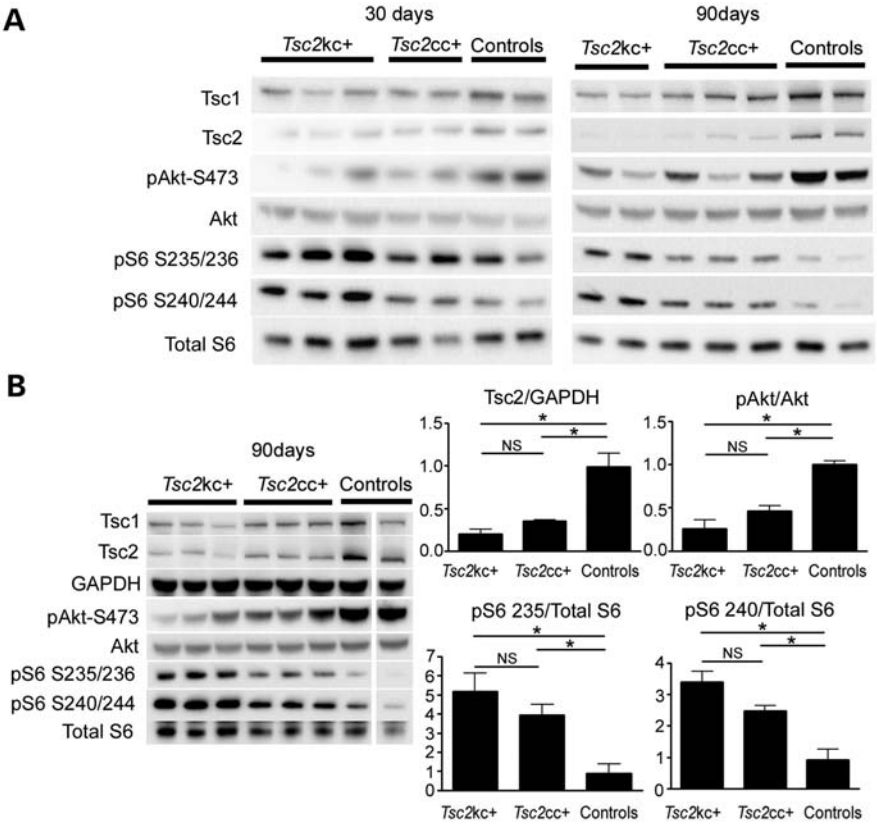

Figure 6. Reduced Tsc2 expression and markers of mTORC1 activation in brain lysates of *Tsc2kc*+ and *Tsc2cc*+ mice. (**A**) Immunoblot analysis of brain lysates from *Tsc2kc*+ and *Tsc2cc*+ mice. Proteins probed are indicated at left; blots on left are from 30-day-old mice; blots on right are from 90-day-old mice. Genotype of controls (from left): 30 days: Tsc2ww+, Tsc2cw−; 90 days: Tsc2cc−, Tsc2cw−. (**B**) Immunoblot and quantitative analysis of brain lysates from 90-day-old *Tsc2kc*+ and *Tsc2cc*+ mice. Immunoblots are shown as in (A). Expression levels of Tsc2 relative to GAPDH, pAkt(S473) relative to Akt, pS6-S235/236 relative to S6 and pS6-S240/244 relative to S6 are shown at right. All ratios for the control samples are normalized to 1. Note that Tsc2:GAPDH levels are markedly reduced, more so in *Tsc2kc*+ lysates, compared with controls, as are pAkt-S473:Akt levels, while pS6-S235/236:S6 and pS6-S240/244:S6 levels are markedly increased. Note that one column of the blot was removed as it was not relevant; all others are from the same blot and exposure. $^{*}P < 0.05$. ns, not significant. All *P*-values by the *t*-test.

(Fig. 6A). Our data on the progressive increase in pS6-S235/236+ neuronal soma size in $Tsc2^{del3/del3}$ and $Tsc2^{k/del3}$ neurons with age (Fig. 3) fit with the inference that as these mutant mice age, the mutant neurons will contribute a greater proportion of cytoplasm to brain lysates, leading to a progressive decline in Tsc2 protein levels in brain lysates from older mice.

Second, we used an independent approach to measure the level of Tsc2 protein expression from the *Tsc2 del3* allele in neurons. We analyzed neuronal cultures from $Tsc2^{c\text{-}del3/c\text{-}del3}$ *Nestin-Cre*+ embryos *in vitro*. The *Nestin-Cre* allele leads to expression of cre recombinase in all neuroprogenitor cells beginning at E8.5 (27,28), making it ideal for this purpose. Immunoblot analysis of neuronal cultures from E17 $Tsc2^{c\text{-}del3/c\text{-}del3}$*Nestin-Cre*+ brains at 7 days *in vitro* showed that Tsc2 expression was 18% of that seen in littermate control neuronal cultures that were *Nestin-Cre* negative (Supplementary Material, Fig. S7). MLPA was used to assess the extent of recombination in the $Tsc2^{c\text{-}del3/c\text{-}del3}$ *Nestin-Cre*+ neuronal cultures, and this was found to be 95%. Therefore, correcting for the contribution of neurons without recombination at the *Tsc2* locus to Tsc2 expression, Tsc2 expression was about 13% of normal levels in the $Tsc2^{del3/del3}$ neurons. These results are clearly very different from our estimate of the level of expression of Tsc2 in brain lysates from *Tsc2cc*+ mice as determined above, 35% of normal. However, considering that the level of recombination in the brain was only 35% of all cells, as determined by MLPA, and hence the large number of cells without recombination in the brain, these values actually are consistent. Thus, we estimate that in *Tsc2cc*+ mutant neurons the level of expression of Tsc2 is 13%, and in the *Tsc2kc*+ neurons it is about 7% of normal.

Tsc2 mutants demonstrate abnormal motor function

Our data thus far have shown a spectrum of worsening phenotypes—brain pathology, decreased survival and limb clasping, with severity corresponding to decreasing levels of Tsc2 protein expression. With their survival and relatively mild phenotype out to age 100 days, *Tsc2kc*+ and *Tsc2cc*+ mice could be studied to examine potential abnormal behaviors representative of the neuropsychiatric phenotypes afflicting TSC patients, in contrast to many previous mouse brain models of TSC.

Patients with TSC have significantly increased rates of attention deficit hyperactivity disorder, characterized by poor

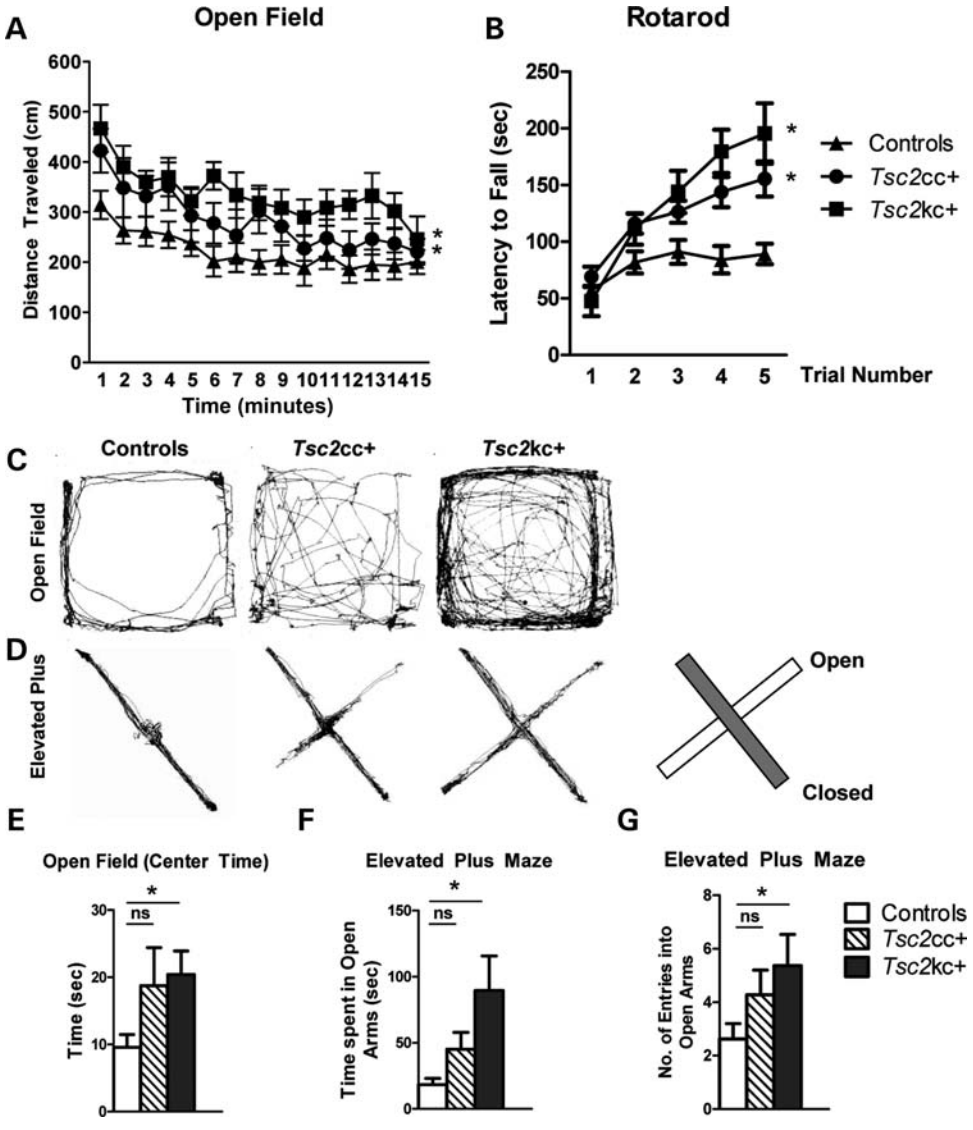

Figure 7. Locomotor activity in Tsc2 mutant mice. (**A**) *Tsc2* mutants display increased distance traveled (cm) in the open field. Time in minutes is shown on the *x*-axis. $^*P < 0.05$ mutant versus control. Total $n = 40$; minimum n per genotype = 8. (**B**) *Tsc2* mutants display increased time on an accelerating rotarod. $^*P < 0.05$ mutant versus control, trials 3–5. Total $n = 25$; minimum n per genotype = 6. $^*P < 0.05$ mutant versus control. (**C** and **D**) Representative open-field (C) and elevated plus maze (D) track plots. Diagram illustrates locations of open and closed arms of the maze. (**E**) *Tsc2kc+* mice display increased time spent in the center quadrant of the open field. Same n as (A). (**F** and **G**) *Tsc2kc+* mice spend more time (F) and enter into the closed arms of the elevated plus maze more frequently (F) in comparison with control littermates. Total $n = 41$; minimum n per genotype = 10. $^*P < 0.05$. ns, not significant. All P-values by the t-test, except open field by ANOVA.

executive functioning, hyperactivity and significantly impulsive behaviors (5). We observed that the mutant mice appeared to be somewhat hyperactive in their cages. Therefore, we quantified the locomotor activity of these mutants using the open-field assay. Both *Tsc2kc+* and *Tsc2cc+* mice demonstrated significantly increased locomotor activity in the open field (Fig. 7A and C, $P = 1.02 \times 10^{-16}$ and 1.8×10^{-5}, respectively), consistent with a hyperactive behavior phenotype. Similar to the previous data, the difference was greatest in the *Tsc2kc+* mice with the *Tsc2cc+* mice demonstrating an intermediate phenotype.

The accelerating rotarod was also used to assess motor performance in the *Tsc2* mutant mice. Both mutants demonstrated similar motor activity to controls on the first day of rotarod trials. However, to our surprise, both *Tsc2kc+* and *Tsc2cc+* mice demonstrated significantly improved motor performance on the rotarod compared with controls in subsequent trials ($P < 0.05$), with an increased latency to falling off in trials 3–5 in comparison with controls. These data suggest improved motor learning in both mutant genotypes, with an increased effect in *Tsc2kc+* mice.

Tsc2 mutants demonstrate abnormal activity in assays for anxiety

Patients with TSC also suffer from high rates of anxiety and mood disorders (29,30). Examination of mouse location during open-field testing suggested that the mutants spent

more time in the center of the open field in comparison with controls (see representative track plots, Fig. 7C). Quantitative analysis showed that this difference between *Tsc2kc+* and control mice was statistically significant (Fig. 7E, $P = 0.008$). *Tsc2cc+* mice spent a similar amount of time in the center of the open field as the *Tsc2kc+* mice, but due to high variance, this increase was not significant in comparison with controls (Fig. 7E, $P = 0.2$). Since rodents normally avoid open spaces, time spent in open areas (center of the open field) can be due to either hyperactivity and/or reduced anxiety.

To evaluate whether mutant animals would demonstrate similar results in other behavioral assessments of anxiety, we tested our animals on the elevated plus maze (31). Similar to the open field, mutant mice demonstrated increased time spent in the open arms of the elevated plus maze, with *Tsc2kc+* mutant mice displaying a significantly increased amount of time ($P = 0.003$, *t*-test) and number of entries ($P = 0.03$) into the open arms (Fig. 7D, F and G). *Tsc2cc+* mice also showed a trend toward increased time spent in the open arms and increased number of entries, but these differences were not significant (Fig. 7D, F and G). Nonetheless, they were clearly intermediate in phenotype between *Tsc2kc+* and control mice.

Taken together, these assays suggest that mutant animals display decreased anxiety as compared with control littermates. However, these assays also rely significantly on motor activity, and an increased impulsive phenotype—consistent with the hyperactivity shown in the open field—could potentially also explain these findings.

Tsc2 mutants demonstrate abnormal social behaviors

Since autism spectrum disorders are also common in TSC (32), we investigated whether mutant mice might also demonstrate autistic-like behaviors. Autism spectrum disorders are marked by three core deficits: social impairment, restrictive behaviors/thinking and abnormal communication. To begin, we tested social interaction in our mouse models using the three-chambered apparatus (33) (see Materials and Methods for details).

In the social approach assay, both *Tsc2kc+* and *Tsc2cc+* mice, similar to controls, demonstrated a significant preference for the novel animal over the novel object both in time spent in the chamber and in interaction with the novel animal (Fig. 8A and C, $P < 0.05$ for each genotype). The amount of time spent in interaction was not statistically different between genotypes ($P > 0.05$), although *Tsc2kc+* mutants demonstrated a trend towards an increased amount of time spent ($P = 0.27$) in the chamber with and interacting with ($P = 0.1$) the novel animal when compared with littermate controls. However, in the social novelty assay, the behavior of the *Tsc2* mutants differed significantly from control littermates. Controls spent significantly more time in the chamber with ($P = 1.0 \times 10^{-7}$) and interacting with ($P = 0.0002$) the novel animal. *Tsc2cc+* mice spent significantly more time in the chamber (Fig. 8B) with the novel animal ($P = 0.038$), but at a reduced level when compared with littermate controls ($P = 0.05$). Examination of the interaction time with the novel animal, however, showed that *Tsc2cc+* mice demonstrated similar rates of interaction when compared with littermate controls (Fig. 8D). *Tsc2kc+* mice, on the other hand, spent similar amounts of time in chambers with both familiar and novel animals ($P = 0.4$), a significant difference from littermate controls in the amount of time spent with the familiar mouse ($P = 0.03$). Similarly, *Tsc2kc+* mice spent as much time interacting with the familiar mouse as with the novel mouse (Fig. 8D, $P = 0.45$), in distinct contrast to both control and *Tsc2cc+* mice. The difference in interaction time with the familiar mouse was highly significant ($P = 0.001$). Thus, social interaction in *Tsc2kc+* mutant mice is clearly abnormal in comparison with littermate controls but appears to be perturbed in a manner distinct from the social avoidance that is commonly observed in patients with autism spectrum disorders. However, some TSC patients show socially inappropriate behaviors such as failing to respect personal distance, which may be consistent with the behavior of the mutant mice seen here.

Tsc2kc+ mice show impaired learning in the water T-maze

In addition, we sought to investigate whether Tsc2 mutant mice demonstrated restrictive behaviors and mental inflexibility, abnormal behaviors seen in patients with ASDs, through use of the reversal learning assay in the water T-maze.

Tsc2kc+ mice demonstrated deficits in the initial learning of the escape platform location (Fig. 8E and F; $P = 0.036$ for number of correct trials, and $P = 0.021$ for number of trials prior to five consecutive correct responses). They showed even greater impairment in finding the escape platform after it was reversed (Fig. 8E and F; $P = 0.0013$ for number of correct trials, $P = 0.0038$ for number of trials prior to five consecutive correct responses). As these animals had impairment in the initial learning phase, it is difficult to distinguish whether their reversal difficulties resulted from perseverative behavior versus visuospatial learning deficits that were magnified in the presence of a more difficult learning paradigm.

We also examined *Tsc2cc+* mice in this reversal learning assay where they showed an intermediate phenotype. They showed no significant impairment in learning the location of the escape platform on days 1–3 (Fig. 8E and F; $P =$ ns for each of number of correct trials, and number of trials prior to five consecutive correct responses). However, when the platform location was reversed, these animals showed impairment in learning the new location on reversal day 1 (Fig. 8E and F; $P = 0.04$ for both number of correct trials, and trials prior to five consecutive responses). These results indicate that although *Tsc2kc+* mice demonstrated impaired acquisition learning, the less severely affected *Tsc2cc+* mutant mice displayed significant impairment only in reversal learning.

DISCUSSION

In this study, we present evidence that graded loss of tuberin in the first allelic series of TSC brain models correlates with survival in addition to biochemical, histological and behavioral features.

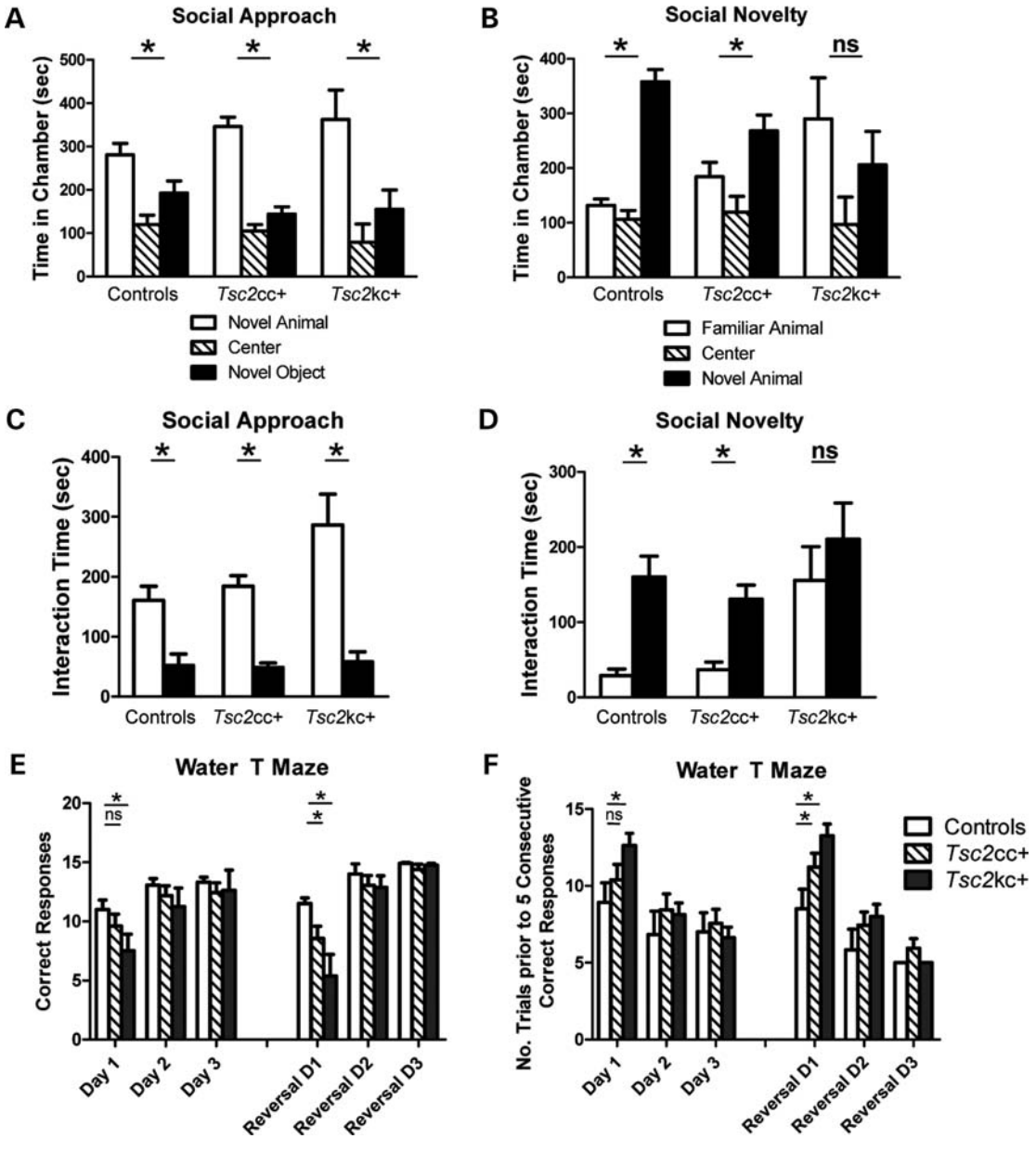

Figure 8. Abnormal social behavior and impaired water T-maze performance in *Tsc2* mutants. (**A** and **C**) In the three-chambered social apparatus, both controls and *Tsc2* mutants spend a greater amount of time in the chamber with the novel animal (A), and more time interacting with the novel animal (C) in comparison with a novel object. Total $n = 39$; minimum n per genotype = 9. (**B** and **D**) *Tsc2kc+* mice show no preference for the chamber with the novel animal in comparison with that with a familiar animal in an assay of social novelty (B), and spend similar time interacting with both the novel and familiar animals (D). This is in distinct contrast to both control and *Tsc2cc+* mice. Same n as (A) and (C). (**E** and **F**) Water T-maze assay. (E) Number of correct trials (out of 15). (F) Number of trials prior to five consecutive correct responses. *Tsc2kc+* mice have significantly fewer correct trials on day 1, and take significantly more trials to achieve five consecutive correct responses on day 1, in comparison with controls. Similarly, they have fewer correct trials after reversal and take longer to achieve five consecutive correct responses on reversal day 1. *Tsc2cc+* mice displayed normal results on day 1, but had significantly fewer correct trials on reversal day 1, and took longer to achieve five consecutive correct responses on reversal day 1. Total $n = 39$; minimum n per genotype = 9. * $P < 0.05$. ns, not significant. All P-values by the t-test.

General phenotype, pathology and expression of Tsc2

For nearly all methods of evaluation of the *Tsc2cc+* and *Tsc2kc+* mice, we observed that the two mutants demonstrated a gradient of severity proportional to the level of expression of Tsc2. *Tsc2*kc+ mice had reduced survival, lower body weights, larger brains and more severe general neurological phenotypes than *Tsc2*cc+ mice (Figs 1 and 2). In comparison with the closely related *Tsc1* model we generated previously, $Tsc1^{cc}SynICre^{+}$ (21), both *Tsc2* mutants demonstrated a much milder phenotype. However, the strains of these two sets of mice were not identical, with both being mixed strains with some shared progenitors, so that formal comparison is not possible. The median survival of *Tsc2*kc+ mice was nearly twice as long as the median survival for the *Tsc1* model (69 days in comparison with 35 days). Neither

of these two hypomorphic *Tsc2* models showed a phenotype prior to age 30 days, while $Tsc1^{cc}SynICre^{+}$ mice had a noticeable phenotype of tremor and poor weight gain beginning at age 10 days (21). We strongly suspect that this difference is due to residual Tsc2 protein expressed in the recombinant neurons in the Tsc2 models, shown here to be 13 and 7%, respectively, in the *Tsc2cc*+ and *Tsc2kc*+ mice, in contrast to complete loss of Tsc1 protein in the $Tsc1^{cc}SynICre^{+}$ mice. However, this level of Tsc2 expression is much lower than what has been reported for $Tsc2^{+/-}$ mouse brains, estimated at about 75% (19). This is consistent with the dramatic increase in pS6-S240/244 levels and reduction in pAKT(S473) levels seen in these models (Fig. 6), in contrast to the absence of such findings in $Tsc2^{+/-}$ mice.

We observed that both *Tsc2*kc+ and *Tsc2*cc+ mice showed increasingly severe neurological symptoms at older ages, though *Tsc2cc*+ mice at age 6 months appeared quite normal in many cases. Although we did not evaluate these mice with electrophysiological monitoring, we suspect that seizures were the cause of death, as clinical seizures were observed on rare occasions, and fatal seizures have been documented in $Tsc1^{cc}SynICre^{+}$ mice (21) and other models (26).

Social and cognitive abnormalities

Patients with TSC have high rates of comorbid neurologic and psychiatric conditions including epilepsy, intellectual disability and attention/hyperactivity disorders (3–6). Previous studies of $Tsc1^{+/-}$ and $Tsc2^{+/-}$ mouse models have demonstrated impairments in hippocampal-dependent learning (19,20), while models in which there is complete loss of Tsc1 or Tsc2 in neurons or astrocytes have had severe phenotypes and reduced survival precluding detailed behavioral assessments (21,22,34).

Our two hypomorphic models demonstrated several abnormal behaviors that are consistent with, while not precisely modeling, those seen in TSC children. In each assay, the phenotype was worse in the *Tsc2kc*+ mice in comparison with the *Tsc2cc*+ mice. Mutants demonstrated markedly increased activity in the open-field test, and increased time and entries into the open arms of the elevated plus assay (Fig. 7). These observations suggest that they had reduced levels of anxiety about exposure, or at least that this response if present was overruled by impulsivity/hyperactivity. They also demonstrated a significant and impressive improvement in rotarod performance with repeated assessments, above that seen in controls (Fig. 7B). The precise cause of this difference is uncertain. It seems possible that it may be related to their hyperactive phenotype seen in the open-field and elevated plus assays, and in their spontaneous increased movement that we have noted in cages.

In the three-chamber assay of social approach, the mutant mice showed similar though slightly increased interaction time with the novel mouse, in comparison with controls, which did not meet statistical significance. However, in the social novelty assay, there was a marked difference in the behavior of the *Tsc2kc*+ mice, which spent a similar amount of time with each of the familiar and the novel mouse (Fig. 8). At face value, this abnormality is clearly different from the abnormal socially isolating behaviors seen in patients with ASDs. However, in other animal models of impaired social behavior (35), animals have demonstrated normal social approach while demonstrating social amnesia in other paradigms. The abnormal behavior seen here in *Tsc2kc*+ animals could be consistent with a deficit in social memory, but is also consistent with impulsivity as seen in the open-field and elevated plus assays.

Both mutants demonstrated abnormal learning and reversal of spatial learning in the water T-maze assay (Fig. 8). Again, deficiencies were greater for the *Tsc2kc*+ than for the *Tsc2cc*+ mice, as learning was not significantly different for the *Tsc2cc*+ mice. These data are consistent with the high rates of learning disability seen in TSC individuals (2,36,37), and previous findings in both $Tsc1^{+/-}$ and $Tsc2^{+/-}$ mice (19,20). This neurocognitive feature also fits with the significant abnormalities seen in the hippocampus of these mutants (Fig. 5, Supplementary Material, Fig. S1). The more severe deficit in reversal learning compared with initial learning seen in both mutants is also consistent with the mental inflexibility characteristic of ASD and obsessive compulsive disorder, both of which are common in patients with TSC (2,37). However, one cannot eliminate the possibility that these data simply reflect learning impairment *per se*, due to the greater difficulty of reversal learning in comparison with initial learning.

Comparison with previous models

Goorden *et al*. (20) were the first to demonstrate significant behavioral abnormalities in any Tsc mouse model, and showed that $Tsc1^{+/-}$ mice displayed social avoidance, reduced nest building and deficits in hippocampal-dependent spatial learning and contextual fear conditioning. Despite these findings, normal anxiety levels were observed in the $Tsc1^{+/-}$ mice, in contrast to our findings. Ehninger *et al*. (19) examined $Tsc2^{+/-}$ mice, and demonstrated learning deficits in three hippocampal-dependent tasks (Morris water maze, eight-arm radial maze and contextual discriminating test), but found normal measures of motor skills, anxiety, exploratory activity and social approach. Young *et al*. (38) performed detailed studies on mother–pup social interaction based on ultrasonic vocalizations, and showed abnormalities in pups born to $Tsc2^{+/-}$ dams. However, $Tsc2^{+/-}$ dams also showed significantly better performance in pup retrieval performance and entries to the nest. These behaviors were described as reminiscent of repetitive, idiosyncratic behavior in ASD patients, who can be extremely focused on certain activities or tasks.

Our findings are more extensive in several respects, and define greater abnormalities, but are overall consistent with these previous studies. The differences among these studies may reflect the effects of the different alleles, and particularly the different genetic backgrounds studied. In the work reported here, it is not surprising that the greater reduction in Tsc2 expression and neuropathological changes would contribute to greater behavioral differences, despite the fact that our studies were performed in a mixed-strain background.

Molecular mechanisms and implications

We found that several biochemical features related to Tsc2 expression as well as overall cellular morphology were altered in a graded manner in these new mutants. Levels of pS6-S240/

244 and pS6-S235/236 relative to S6 were increased about 3-fold and 5-fold, respectively, in brain lysates from *Tsc2kc+* mice; while levels of pAKT(S473) were decreased by about 75% (Fig. 6B). These findings reflect the well-known function of the TSC1–TSC2 protein complex in the regulation of mTORC1 (14,15). However, this is the first study in a brain model of TSC to demonstrate that these signaling and biochemical changes occur in a manner that is proportional to the level of reduction in Tsc2 protein expression, and correlate with neurocognitive and behavioral phenotypes.

In TSC, there is ongoing study to try to distinguish the relative contributions of several different aspects of brain pathology to the observed clinical phenotype (4,5,39). Potential contributors to pathophysiology in TSC include: global effects of loss of one functional allele of TSC1 or TSC2 resulting in diminished protein levels in all cells, haploinsufficiency, leading to both reduced protein synthesis and a deficit in synaptic plasticity; effects of putative two hit complete loss of TSC1 or TSC2 expression in tuber giant and dysmorphic cells (40,41); effects of cortical disruption seen in regions near tubers; effects of early onset and often refractory epilepsy (42); and aberrant connectivity in the white matter as defined by diffusion tensor imaging (18). It is likely that all of these contribute to intellectual outcome, neurocognitive and behavioral problems in TSC patients. Previous studies (19,20,38) as well as our findings indicate that reduction in the expression of Tsc1/Tsc2 in the mouse brain leads to significant neurocognitive and behavioral effects. Furthermore, the graded differences in behavioral abnormalities seen in these new models are consistent with evidence that neurocognitive outcomes including intellectual disability are improved in TSC individuals with higher levels of expression of TSC1/TSC2 globally in the brain. Such evidence includes: the finding that TSC subjects with TSC1 mutations have better intellectual outcomes than those with TSC2 mutations, in which there may be improved function due to higher levels of TSC2 (43); individuals with missense mutations in TSC2 have better intellectual outcomes than those with truncating mutations in TSC2 (44); and individuals with mosaicism for a TSC gene mutation, who have a proportion of brain cells with two normal alleles, also have a better outcome (45). Moreover, these observations in aggregate suggest that approaches which increase the level of expression of the TSC1/TSC2 protein complex by whatever means in brain cells may have therapeutic benefit in leading towards more normal neurocognitive function in TSC individuals. Currently, there are limited methods to achieve this goal, but future research may enable such a possibility, including methods for getting 'read through' to suppress nonsense mutations, improving the stability and function of TSC2 proteins containing missense mutations, and enhancement of mRNA and/or protein production from the remaining wild-type allele.

Everolimus or rapamycin has been shown to have benefit in the treatment of several tumors that occur in TSC: renal angiomyolipomas, pulmonary lymphangioleiomyomatosis and subependymal giant cell astrocytomas (46–48). These agents are now being explored for treatment of neurobehavioral phenotypes in TSC as well. A treatment approach that is in some ways equivalent to increasing expression of TSC2 in the brain is treatment with everolimus/rapamycin at a low level, sufficient to restore mTORC1 signaling to some extent, while avoiding side effects and reducing long-term risk. Thus, our findings also suggest that this therapeutic approach may have benefit.

MATERIALS AND METHODS

Mouse alleles, breeding strategy and phenotyping

All mouse procedures were performed in accordance with the *Guide for the Humane Use and Care of Laboratory Animals*, and the study was approved by the Animal Care and Use Committee of Children's Hospital Boston.

Mouse experiments were performed in a mixed-strain background. $Tsc2^{k}$ and $Tsc2^{c\text{-}del3}$ alleles were previously generated and described (24,49). $Tsc2^{k}$ is a null or knockout allele of *Tsc2* from which there is no protein expression (49). $Tsc2^{c\text{-}del3}$ is a conditional allele of *Tsc2* that has normal expression of Tsc2 until cre-mediated recombination converts it to a $Tsc2^{del3}$ allele, from which low levels of del3-Tsc2 protein is expressed (24). The *SynICre* allele was brought in from our existing colony of $Tsc1^{c/c}SynIcre^{+}$ mice, and in aggregate, this mixed strain has a similar genetic background to that of the $Tsc1^{c/c}SynIcre^{+}$ mice.

We created a mixed common breeding colony to generate mice with the genotypes $Tsc2^{c\text{-}del3/c\text{-}del3}SynICre^{+}$ and $Tsc2^{k/c\text{-}del3}$ $SynICre^{+}$. Control mice in each experiment were gender-matched littermates of the mutants being studied. Control genotypes included: $Tsc2^{w/w}SynICre^{-}$, $Tsc2^{w/w}$ $SynICre^{+}$, $Tsc2^{c\text{-}del3/w}SynICre^{-}$, $Tsc2^{c\text{-}del3/c\text{-}del3}SynICre^{-}$, $Tsc2^{c\text{-}del3/w}SynICre^{+}$ and $Tsc2^{k/c\text{-}del3}SynICre^{-}$. The last two genotypes were not used as controls for behavioral studies.

We also generated mice with the genotype $Tsc2^{c\text{-}del3/c\text{-}del3}$ *Nestin-Cre+* (27) and littermate controls, for *in vitro* studies of neuronal culture. The *Rosa26LacZ* reporter was used as a marker allele for Cre-mediated recombination (50).

Phenotype scoring was performed by an observer blinded to genotype. Hunchback was scored as: 1, normal; 2, present, mild to moderate; 3, severe, such that it was easily recognized. Hind limb strain was determined by suspending the mouse in the air by the tail and was scored as follows: 1, normal lateral spread of hind limbs; 2, hind limb shaking and out-of-plane movement; 3, hind limb movement toward midline; 4, clasping of hind limbs. Straub tail was scored as present if the tail was held tonically at an angle $>0^{\circ}$ relative to the surface. Tremor was scored as absent or present in the absence of stimulation or handling.

DNA analyses—genotyping and MLPA

The *Tsc2 c-del3*, *del3* and *w* alleles were genotyped by PCR using a three-primer reaction that detected all three alleles, as described (24). The separate *Tsc2 k* and *w* alleles were genotyped in separate PCR reactions as described (49). The *Cre* allele was genotyped by standard means (51).

Multiplex ligation-dependent probe amplification (MLPA) was used to quantitatively measure the amount of the *c-del3* and *del3* alleles of *Tsc2* in a DNA preparation. For MLPA analysis, DNA was prepared from mouse brain cortex and other sources (mouse tail or toe) using the PUREGENE DNA

purification kit (Gentra/Qiagen). MLPA probes were designed based upon the native sequence of the *Tsc2* allele, and the modified sequence present in the $Tsc2^{c\text{-}del3}$ and $Tsc2^{del3}$ alleles (52) (Supplementary Material, Fig. S5). The MLPA reaction was performed using reaction kits from MRC-Holland, and products were analyzed by capillary electrophoresis. Peak heights were determined using GeneImager v. 2 (ABI). The relative amounts of $Tsc2^{c\text{-}del3}$ and $Tsc2^{del3}$ alleles were determined by normalization to these values from $Tsc2^{c\text{-}del3/del3}$ samples.

Histological analyses

Brains and spinal cords were prepared for routine staining and immunostaining by fixation in Bouin's solution (Sigma-Aldrich). H&E-stained brain sections were used to measure neuron soma size as described previously (21). These analyses were performed on the M1 region of the cortex on coronal sections containing the anterior region of the hippocampus. Two or more mice were analyzed ($n \geq 2$) for all cohorts and age groups. Similar methods were used for the measurement of anterior horn motor neurons in the spinal cord, with the modification that the three largest neurons at each level (cervical, thoracic, lumbar and sacral) were measured.

LacZ staining was performed on 20 μm frozen brain sections after 1 h fixation in 1% paraformaldehyde, as described previously (21).

Immunohistochemistry

Brain and spinal cord sections for immunohistochemistry were initially deparaffinized through xylene and alcohol series, treated with Target Retrieval Solution pH 6.1 (Dako), followed by blocking in 3% H_2O_2 in methanol and then in 5% normal goat serum in 0.1% Triton X in PBS. Slides were incubated with primary antibodies overnight at 4°C, rinsed and treated with anti-rabbit secondary antibody conjugated with horseradish peroxidase, followed by DAB substrate for color reaction development (Dako Envision System). Slides were counterstained with hematoxylin (Dako). Antibodies used for staining were: anti-pS6-S235/236 (1:1000, Cell Signaling, no. 2211) and anti-tuberin (1:200, Cell Signaling, no. 4308).

Immunoblotting

Mouse brains were harvested for immunoblotting by rapid freezing in liquid nitrogen and stored at −80°C until further use. Small portions (<10%) of the cerebral cortex from some of these brains were used for DNA isolation, as above. Lysates from brain samples were prepared by standard methods (21). Neuronal lysates from cultures were harvested using cell lysis buffer (Cell Signaling Technology, Bedford, MA, USA). Antibodies used for western blotting were as follows: Tsc2 and Akt (Santa Cruz Biotechnology, Santa Cruz, CA, USA); pS6-S240/244, pS6-S235/236, total S6 and Tsc1 (Cell Signaling Technology); pAkt(S473) (Dako); and GAPDH (Abcam). Blotting signal was collected digitally using the Syngene G-box iChemi XT GeneSnap program (Version 7.09.06). Densitometry measurements were performed using the Syngene GeneTools (Version 4.01.02) program. Signal intensities were calculated with subtraction of background signal, and normalized to both control samples and control proteins (pAkt to Akt; pS6-S240/244 and pS6-S235/236 to total S6; Tsc2 to GAPDH or Akt). Immunoblotting results were always performed in at least triplicate; representative images are shown.

Neuronal culture

Timed matings between female $Tsc2^{c\text{-}del3/c\text{-}del3}$*Nestin-Cre*− and male $Tsc2^{c\text{-}del3/w}$*Nestin-Cre*+ were used to collect embryos at embryonic day 17 for neuronal culture. Brains were suspended in HBSS containing 10 mM $MgCl_2$, 1 mM kynurenic acid, 10 mM HEPES and penicillin/streptomycin, incubated in 30 U/ml papain (Worthington) for 5 min and then mechanically triturated and plated in Neurobasal medium containing B27 supplement, 2 mM L-glutamine and penicillin/streptomycin (Gibco/Invitrogen). Cells from each mouse brain were plated in a different 10 cm plate coated with 20 μg/ml poly-D-lysine. Neuronal cultures were harvested for immunoblotting and MLPA after 7 days *in vitro.* These media select for neuronal growth, and based upon morphologic characteristics, >99% of these cells were neurons.

Behavioral analyses

Behavioral analyses were initiated at age 6 weeks, and completed by 8.5 weeks of age for all mice. They were performed in a fixed sequential manner at the same timepoint in the circadian cycle for all mice. All assays were done by the same investigators (P.T.T. or E.G.-C.), blinded to genotype and running experiments on groups of animals of all genotypes on the same day. Both female and male mice were studied, of approximately equal numbers for each genotype and test.

Water T-maze

Reversal learning was tested using the water T-maze as described (53) on mice of age 8 weeks. Briefly, animals were placed in a T-shaped apparatus filled with water (at 23°C). On day (D) 0, mice were habituated to the apparatus for a 60 s period. On D1–3, mice were given 15 trials, with one trial every 5 min. In each trial, mice were placed in the stem of the T apparatus and allowed to swim freely. Mice were given up to 35 s to locate a submerged platform placed on one of the arms of the T. Once the platform was located, the animals were allowed to stay on the platform for 15 s prior to being returned to their cages. If the mouse did not find the platform in 35 s, it was then placed on the platform for 15 s prior to being returned to the cage. Mice were allowed to recover under indirect heat for 3 min after each test prior to the next trial. After 15 trials on D3, animals were given a 10 min break. During the break, the platform was changed to the other T arm. Mice were then tested for an additional 15 trials as above. The number of correct trials was recorded for each mouse, as well as the number of trials needed prior to achieving five consecutive correct trials.

Social interaction

Animals were tested for social interaction as previously described (33). Animals were tested in a three-chamber

apparatus. Animals were initially habituated to the apparatus. After habituation, animals were placed individually into the middle chamber while a novel male animal was placed into an inverted wire cup (novel animal) in one side chamber while an empty wire cup (novel object) was placed into the other side chamber. The tested animal was then allowed to explore the apparatus for a 10 min trial. Time in each chamber was recorded in an automated manner (National Instruments), while time spent interacting with the novel animal and the object was recorded by the examiner. After the 10 min trial, the animal was returned to the middle chamber while another unfamiliar age-matched male animal (novel animal) was placed under the previously empty wire cup. The tested animal was then allowed to explore the apparatus for an additional 10 min trial, and time in each chamber and time spent interacting with the novel and familiar animals were recorded as above. Animals were tested at 7 weeks of age.

Open field
Open-field testing was performed as described (54). Mice were placed in a brightly lit square (44 × 44 cm) arena, and allowed to move freely for 15 min. Mice had not previously been exposed to this device. Movement and time spent in center quadrants were recorded by camera and analyzed by Noldus analysis software. Measurements were taken on 7-week-old mice.

Elevated plus maze
Elevated plus maze testing was performed as described (31). Briefly, mice were placed in the center of the elevated plus maze apparatus for a 5 min trial. Mouse movements were recorded with Noldus software. Mice were determined to be on an open arm when all four limbs were fully on the open arm. Mice were tested at 7 weeks of age.

Rotarod
Animals were tested using the accelerating rotarod as described (55). Animals were placed on the rotarod at a starting rotational velocity of 4 rpm, which then accelerated to 40 rpm over a period of 5 min. Latency to fall was recorded. Animals were given multiple trials per day over 5 consecutive days. Animals were tested at 6 weeks of age.

Statistical analyses

Statistical analyses were performed using the Prism4 program (GraphPad Sofware Inc.). A P-value <0.05 was considered significant. Statistical analysis of survival curves was performed using the Mantel–Haenszel test. Statistical analyses of differences between groups of animals in body weight, brain weight and neuron soma size were determined by the Mann–Whitney non-parametric test. These data are reported as mean ± SD. Pair-wise comparisons of the $Tsc2^{c\text{-}del3/c\text{-}del3}$ SynICre^{+} and its control cohort, and of the $Tsc2^{k/c\text{-}del3}$ SynICre^{+} and its control cohort, were made at each time point. Statistical analysis of the percent recombination in brain cells among different groups was determined by one-way ANOVA. Immunoblot data on neuronal expression were analyzed using the two-tailed unpaired t-test. For behavioral assays, data are reported as mean ± SEM, and statistical analysis was carried out using Student's t-test (two-tailed, unpaired). Repeated-measures two-way ANOVA was performed for open-field test analysis.

SUPPLEMENTARY MATERIAL

Supplementary Material is available at *HMG* online.

ACKNOWLEDGEMENTS

The authors wish to thank June Goto and Alessia di Nardo for assistance with neuronal culture.

Conflict of Interest statement. None declared.

FUNDING

This work was supported by National Institutes of Health (1P01NS24279-16, 2R37NS031535-14). P.T.T. received support from the Developmental Neurology Training Grant (T32 NS007473), American Academy of Neurology and the Nancy Lurie Marks Family Foundation. M.S. was supported by the John Merck Scholars Fund and the Children's Hospital Boston Translational Research Program.

REFERENCES

1. Kwiatkowski, D.J., Thiele, E.A. and Whittemore, V.H. (2010) *Tuberous Sclerosis Complex*. Wiley-VCH, Weinheim, Germany.
2. Thiele, E.A. and Jozwiak, S. (2010) Natural history of tuberous sclerosis complex and overview of manifestations. In Kwiatkowski, D.J., Whittemore, V.H. and Thiele, E.A. (eds.), *Tuberous Sclerosis Complex*. Wiley-VCH, Weinheim, Germany, pp. 11–20.
3. Winterkorn, E.B., Pulsifer, M.B. and Thiele, E.A. (2007) Cognitive prognosis of patients with tuberous sclerosis complex. *Neurology*, **68**, 62–64.
4. Tierney, K.M., McCartney, D.L., Serfontein, J.R. and de Vries, P.J. (2011) Neuropsychological attention skills and related behaviours in adults with tuberous sclerosis complex. *Behav. Genet.*, **41**, 437–444.
5. Yates, J.R., Maclean, C., Higgins, J.N., Humphrey, A., le Marechal, K., Clifford, M., Carcani-Rathwell, I., Sampson, J.R. and Bolton, P.F. (2011) The Tuberous Sclerosis 2000 Study: presentation, initial assessments and implications for diagnosis and management. *Arch. Dis. Child.*, **96**, 1020–1025.
6. Gutierrez, G.C., Smalley, S.L. and Tanguay, P.E. (1998) Autism in tuberous sclerosis complex. *J. Autism. Dev. Disord.*, **28**, 97–103.
7. Sampson, J.R., Scahill, S.J., Stephenson, J.B., Mann, L. and Connor, J.M. (1989) Genetic aspects of tuberous sclerosis in the west of Scotland. *J. Med. Genet.*, **26**, 28–31.
8. Kwiatkowski, D.J. (2010) Genetics of tuberous sclerosis complex. In Kwiatkowski, D.J., Whittemore, V.H. and Thiele, E.A. (eds), *Tuberous Sclerosis Complex: Genes, Clinical Features, and Therapeutics*. Wiley-VCH, Winheim, pp. 29–59.
9. Nellist, M., Sancak, O., Goedbloed, M., Adriaans, A., Wessels, M., Maat-Kievit, A., Baars, M., Dommering, C., van den Ouweland, A. and Halley, D. (2008) Functional characterisation of the TSC1–TSC2 complex to assess multiple TSC2 variants identified in single families affected by tuberous sclerosis complex. *BMC Med. Genet.*, **9**, 10.
10. Jansen, A.C., Sancak, O., D'Agostino, M.D., Badhwar, A., Roberts, P., Gobbi, G., Wilkinson, R., Melanson, D., Tampieri, D., Koenekoop, R. *et al.* (2006) Unusually mild tuberous sclerosis phenotype is associated with TSC2 R905Q mutation. *Ann. Neurol.*, **60**, 528–539.
11. O'Connor, S.E., Kwiatkowski, D.J., Roberts, P.S., Wollmann, R.L. and Huttenlocher, P.R. (2003) A family with seizures and minor features of tuberous sclerosis and a novel TSC2 mutation. *Neurology*, **61**, 409–412.

12. Khare, L., Strizheva, G.D., Bailey, J.N., Au, K.S., Northrup, H., Smith, M., Smalley, S.L. and Henske, E.P. (2001) A novel missense mutation in the GTPase activating protein homology region of TSC2 in two large families with tuberous sclerosis complex. *J. Med. Genet.*, **38**, 347–349.
13. Wentink, M., Nellist, M., Hoogeveen-Westerveld, M., Zonnenberg, B., van der Kolk, D., van Essen, T., Park, S.M., Woods, G., Cohn-Hokke, P., Brussel, W. *et al.* (2011) Functional characterization of the TSC2 c.3598C>T (p.R1200W) missense mutation that co-segregates with tuberous sclerosis complex in mildly affected kindreds. *Clin. Genet.*, 10.1111/j.1399–0004.2011.01648.x.
14. Yecies, J.L. and Manning, B.D. (2011) mTOR links oncogenic signaling to tumor cell metabolism. *J. Mol. Med.*, **89**, 221–228.
15. Zoncu, R., Efeyan, A. and Sabatini, D.M. (2011) mTOR: from growth signal integration to cancer, diabetes and ageing. *Nat. Rev. Mol. Cell. Biol.*, **12**, 21–35.
16. Hsu, P.P., Kang, S.A., Rameseder, J., Zhang, Y., Ottina, K.A., Lim, D., Peterson, T.R., Choi, Y., Gray, N.S., Yaffe, M.B. *et al.* (2011) The mTOR-regulated phosphoproteome reveals a mechanism of mTORC1-mediated inhibition of growth factor signaling. *Science*, **332**, 1317–1322.
17. Yu, Y., Yoon, S.O., Poulogiannis, G., Yang, Q., Ma, X.M., Villen, J., Kubica, N., Hoffman, G.R., Cantley, L.C., Gygi, S.P. *et al.* (2011) Phosphoproteomic analysis identifies Grb10 as an mTORC1 substrate that negatively regulates insulin signaling. *Science*, **332**, 1322–1326.
18. Tsai, P. and Sahin, M. (2011) Mechanisms of neurocognitive dysfunction and therapeutic considerations in tuberous sclerosis complex. *Curr. Opin. Neurol.*, **24**, 106–113.
19. Ehninger, D., Han, S., Shilyansky, C., Zhou, Y., Li, W., Kwiatkowski, D.J., Ramesh, V. and Silva, A.J. (2008) Reversal of learning deficits in a Tsc2(+/−) mouse model of tuberous sclerosis. *Nat. Med.*, **14**, 843–848.
20. Goorden, S.M., van Woerden, G.M., van der Weerd, L., Cheadle, J.P. and Elgersma, Y. (2007) Cognitive deficits in Tsc1+/− mice in the absence of cerebral lesions and seizures. *Ann. Neurol.*, **62**, 648–655.
21. Meikle, L., Talos, D.M., Onda, H., Pollizzi, K., Rotenberg, A., Sahin, M., Jensen, F.E. and Kwiatkowski, D.J. (2007) A mouse model of tuberous sclerosis: neuronal loss of Tsc1 causes dysplastic and ectopic neurons, reduced myelination, seizure activity, and limited survival. *J. Neurosci.*, **27**, 5546–5558.
22. Uhlmann, E.J., Wong, M., Baldwin, R.L., Bajenaru, M.L., Onda, H., Kwiatkowski, D.J., Yamada, K. and Gutmann, D.H. (2002) Astrocyte-specific TSC1 conditional knockout mice exhibit abnormal neuronal organization and seizures. *Ann. Neurol.*, **52**, 285–296.
23. Way, S.W., McKenna, J. 3rd, Mietzsch, U., Reith, R.M., Wu, H.C. and Gambello, M.J. (2009) Loss of Tsc2 in radial glia models the brain pathology of tuberous sclerosis complex in the mouse. *Hum. Mol. Genet.*, **18**, 1252–1265.
24. Pollizzi, K., Malinowska-Kolodziej, I., Doughty, C., Betz, C., Ma, J., Goto, J. and Kwiatkowski, D.J. (2009) A hypomorphic allele of Tsc2 highlights the role of TSC1/TSC2 in signaling to AKT and models mild human TSC2 alleles. *Hum. Mol. Genet.*, **18**, 2378–2387.
25. Zhu, Y., Romero, M.I., Ghosh, P., Ye, Z., Charnay, P., Rushing, E.J., Marth, J.D. and Parada, L.F. (2001) Ablation of NF1 function in neurons induces abnormal development of cerebral cortex and reactive gliosis in the brain. *Genes Dev.*, **15**, 859–876.
26. Goto, J., Talos, D.M., Klein, P., Qin, W., Chekaluk, Y.I., Anderl, S., Malinowska, I.A., Di Nardo, A., Bronson, R.T., Chan, J.A. *et al.* (2011) Regulable neural progenitor-specific Tsc1 loss yields giant cells with organellar dysfunction in a model of tuberous sclerosis complex. *Proc. Natl. Acad. Sci. USA*, **108**, E1070–E1079.
27. Tronche, F., Kellendonk, C., Kretz, O., Gass, P., Anlag, K., Orban, P.C., Bock, R., Klein, R. and Schutz, G. (1999) Disruption of the glucocorticoid receptor gene in the nervous system results in reduced anxiety. *Nat. Genet.*, **23**, 99–103.
28. Anderl, S., Freeland, M., Kwiatkowski, D.J. and Goto, J. (2011) Therapeutic value of prenatal rapamycin treatment in a mouse brain model of tuberous sclerosis complex. *Hum. Mol. Genet.*, **20**, 4597–4604.
29. de Vries, P.J., Hunt, A. and Bolton, P.F. (2007) The psychopathologies of children and adolescents with tuberous sclerosis complex (TSC): a postal survey of UK families. *Eur. Child. Adolesc. Psychiatry*, **16**, 16–24.
30. Muzykewicz, D.A., Newberry, P., Danforth, N., Halpern, E.F. and Thiele, E.A. (2007) Psychiatric comorbid conditions in a clinic population of 241 patients with tuberous sclerosis complex. *Epilepsy Behav.*, **11**, 506–513.
31. Hogg, S. (1996) A review of the validity and variability of the elevated plus-maze as an animal model of anxiety. *Pharmacol. Biochem. Behav.*, **54**, 21–30.
32. Hunt, A. and Shepherd, C. (1993) A prevalence study of autism in tuberous sclerosis. *J. Autism Dev. Disord.*, **23**, 323–339.
33. Silverman, J.L., Yang, M., Lord, C. and Crawley, J.N. (2010) Behavioural phenotyping assays for mouse models of autism. *Nat. Rev. Neurosci.*, **11**, 490–502.
34. Zeng, L.H., Rensing, N.R., Zhang, B., Gutmann, D.H., Gambello, M.J. and Wong, M. (2011) Tsc2 gene inactivation causes a more severe epilepsy phenotype than Tsc1 inactivation in a mouse model of tuberous sclerosis complex. *Hum. Mol. Genet.*, **20**, 445–454.
35. Ferguson, J.N., Young, L.J., Hearn, E.F., Matzuk, M.M., Insel, T.R. and Winslow, J.T. (2000) Social amnesia in mice lacking the oxytocin gene. *Nat. Genet.*, **25**, 284–288.
36. Prather, P. and de Vries, P.J. (2004) Behavioral and cognitive aspects of tuberous sclerosis complex. *J. Child. Neurol.*, **19**, 666–674.
37. Pulsifer, M.B., Winterkorn, E.B. and Thiele, E.A. (2007) Psychological profile of adults with tuberous sclerosis complex. *Epilepsy Behav.*, **10**, 402–406.
38. Young, D.M., Schenk, A.K., Yang, S.B., Jan, Y.N. and Jan, L.Y. (2010) Altered ultrasonic vocalizations in a tuberous sclerosis mouse model of autism. *Proc. Natl. Acad. Sci. U S. A.*, **107**, 11074–11079.
39. Numis, A.L., Major, P., Montenegro, M.A., Muzykewicz, D.A., Pulsifer, M.B. and Thiele, E.A. (2011) Identification of risk factors for autism spectrum disorders in tuberous sclerosis complex. *Neurology*, **76**, 981–987.
40. Qin, W., Chan, J.A., Vinters, H.V., Mathern, G.W., Franz, D.N., Taillon, B.E., Bouffard, P. and Kwiatkowski, D.J. (2010) Analysis of TSC cortical tubers by deep sequencing of TSC1, TSC2 and KRAS demonstrates that small second-hit mutations in these genes are rare events. *Brain Pathol.*, **20**, 1096–1105.
41. Crino, P.B., Aronica, E., Baltuch, G. and Nathanson, K.L. (2010) Biallelic TSC gene inactivation in tuberous sclerosis complex. *Neurology*, **74**, 1716–1723.
42. Chu-Shore, C.J., Major, P., Camposano, S., Muzykewicz, D. and Thiele, E.A. (2010) The natural history of epilepsy in tuberous sclerosis complex. *Epilepsia*, **51**, 1236–1241.
43. Dabora, S.L., Jozwiak, S., Franz, D.N., Roberts, P.S., Nieto, A., Chung, J., Choy, Y.S., Reeve, M.P., Thiele, E., Egelhoff, J.C. *et al.* (2001) Mutational analysis in a cohort of 224 tuberous sclerosis patients indicates increased severity of TSC2, compared with TSC1, disease in multiple organs. *Am. J. Hum. Genet.*, **68**, 64–80.
44. van Eeghen, A.M., Black, M.E., Pulsifer, M.B., Kwiatkowski, D.J. and Thiele, E.A. (2012) Genotype and cognitive phenotype of patients with tuberous sclerosis complex. *Eur. J. Hum. Genet.*, **20**, 510–5.
45. Verhoef, S., Bakker, L., Tempelaars, A.M., Hesseling-Janssen, A.L., Mazurczak, T., Jozwiak, S., Fois, A., Bartalini, G., Zonnenberg, B.A., van Essen, A.J. *et al.* (1999) High rate of mosaicism in tuberous sclerosis complex. *Am. J. Hum. Genet.*, **64**, 1632–1637.
46. Bissler, J.J., McCormack, F.X., Young, L.R., Elwing, J.M., Chuck, G., Leonard, J.M., Schmithorst, V.J., Laor, T., Brody, A.S., Bean, J. *et al.* (2008) Sirolimus for angiomyolipoma in tuberous sclerosis complex or lymphangioleiomyomatosis. *N. Engl. J. Med.*, **358**, 140–151.
47. McCormack, F.X., Inoue, Y., Moss, J., Singer, L.G., Strange, C., Nakata, K., Barker, A.F., Chapman, J.T., Brantly, M.L., Stocks, J.M. *et al.* (2011) Efficacy and safety of sirolimus in lymphangioleiomyomatosis. *N. Engl. J. Med.*, **364**, 1595–1606.
48. Krueger, D.A., Care, M.M., Holland, K., Agricola, K., Tudor, C., Mangeshkar, P., Wilson, K.A., Byars, A., Sahmoud, T. and Franz, D.N. (2010) Everolimus for subependymal giant-cell astrocytomas in tuberous sclerosis. *N. Engl. J. Med.*, **363**, 1801–1811.
49. Onda, H., Lueck, A., Marks, P.W., Warren, H.B. and Kwiatkowski, D.J. (1999) Tsc2(+/−) mice develop tumors in multiple sites that express gelsolin and are influenced by genetic background. *J. Clin. Invest.*, **104**, 687–695.
50. Soriano, P. (1999) Generalized lacZ expression with the ROSA26 Cre reporter strain. *Nat. Genet.*, **21**, 70–71.
51. Meikle, L., McMullen, J.R., Sherwood, M.C., Lader, A.S., Walker, V., Chan, J.A. and Kwiatkowski, D.J. (2005) A mouse model of cardiac

rhabdomyoma generated by loss of Tsc1 in ventricular myocytes. *Hum. Mol. Genet.*, **14**, 429–435.
52. Kozlowski, P., Roberts, P., Dabora, S., Franz, D., Bissler, J., Northrup, H., Au, K.S., Lazarus, R., Domanska-Pakiela, D., Kotulska, K. *et al.* (2007) Identification of 54 large deletions/duplications in TSC1 and TSC2 using MLPA, and genotype–phenotype correlations. *Hum. Genet.*, **121**, 389–400.
53. Bednar, I., Paterson, D., Marutle, A., Pham, T.M., Svedberg, M., Hellstrom-Lindahl, E., Mousavi, M., Court, J., Morris, C., Perry, E. *et al.* (2002) Selective nicotinic receptor consequences in APP(SWE) transgenic mice. *Mol. Cell. Neurosci.*, **20**, 354–365.
54. Holmes, A., Wrenn, C.C., Harris, A.P., Thayer, K.E. and Crawley, J.N. (2002) Behavioral profiles of inbred strains on novel olfactory, spatial and emotional tests for reference memory in mice. *Genes Brain Behav.*, **1**, 55–69.
55. Buitrago, M.M., Schulz, J.B., Dichgans, J. and Luft, A.R. (2004) Short and long-term motor skill learning in an accelerated rotarod training paradigm. *Neurobiol. Learn. Mem.*, **81**, 211–216.